Progress In Electromagnetics Research M, Vol. 39, 141–150, 2014

Kriging-Pareto Front Approach for the Multi-Objective Exploration of Metamaterial Topologies

Patrick J. Bradley*

Abstract—Metamaterials provide the opportunity for designers to create customisable artificial materials by independently tailoring the electric and magnetic response of sub-wavelength geometric structures to electromagnetic energy. Due to the increased complexity of these geometric structures, exacerbated by the increased interest in generating inhomogeneous and anisotropic metamaterials, direct optimisation of these designs using conventional approaches often becomes impractical and limited. In order to alleviate this issue, we propose an alternative optimisation approach which exploits the Kriging methodology in conjunction with an adaptive sampling plan to simultaneously optimise multiple conflicting objectives. Results show the effectiveness of the outlined algorithm in calculating a uniform spread of optimal trade-off designs, balancing the real and imaginary components of the refractive index over a wide range of values.

1. INTRODUCTION

The realisation of ever more complicated optical transformation designs has driven the need for a wider range of inhomogeneous and anisotropic metamaterial structures. This growth in complexity of the electromagnetic properties, coupled with the need to often balance several goals simultaneously, requires a fresh approach that can provide an accessible and systematic approach to the design of complex metamaterial structure. This is in part due to the inherently high computational cost associated with running multiple expensive high-fidelity full-wave simulations, commonly required to optimise the constitutive parameters of a single metamaterial particle. Additionally, this is often coupled with underlying numerical noise that can adversely affect the simulation-driven optimisation cycle. Thus, a key challenge is to be able to perform global optimisation using physics-based simulations in an efficient manner so as to allow these methods to be used within the short time-scales of conceptual design. As such there is a need to devise an automated and rapid method to obtain the optimised geometric parameters for metamaterial design to satisfy a range of desired material responses. These structures can then be incorporated in to a system level design that can be used in devices ranging from gradient index lens to metamaterial polarizers [1, 2].

In this work, we prioritise the simultaneous optimisation of the real part and imaginary component of the refractive index. These aspirations are clearly conflicting with each other and so compromise solutions have to be sought. One approach is to reduce the problem from one with multiple goals to a single objective problem by using suitable weighting functions that combine the goals of interest [3]. However, the correct weighting to apply between goals is not always obvious or the designer does not wish to commit to a fixed weighting while carrying out design searches. This leads to the concept of Pareto optimality [4, 5] and sets of designs that must be found and considered simultaneously. Construction of a Pareto fronts is associated to solving a Multi-Objective (MO) problem [5, 6]. Each point on this front represents one solution in the objective solution space of the MO problem and has an associated

Received 12 September 2014, Accepted 22 October 2014, Scheduled 3 November 2014
* Corresponding author: Patrick J. Bradley (bradleypatrickj@gmail.com).
The author is with the RF & Microwave Research Group, School of Electrical Electronic and Communications Engineering, University College Dublin, Ireland.

set of design variables stored in the Pareto set. A Pareto set of designs is one whose members are all optimal in some sense. An improvement in the performance of any set member, in any one goal function, involves the deterioration of the others [7]. Moreover, the designs in the set are said to be non-dominating, in that no other set member exceeds a given designs performance in all goals.

The construction of a Pareto front can be very complex especially in the presence of a multi-modal objective function. Currently there are two popular approaches to constructing these sets, stochastic optimizers or statistically based operators [5, 8, 9]. Stochastic approaches developed in the past decade are good for achieving a well-distributed solution at the expense of a large computational effort. While these expenses can be mitigated by using surrogate based modelling techniques these approaches still suffer from an inability to explicitly balance exploration and exploitation of the surrogate model construction [5]. Here, we will consider statistically based operators for use in surrogate model based multi-objective search so as to explicably tackle these problems. Central to the success of our approach will be the inclusions of the Multi-Objective Expected Improvement (MOEI) criteria [4–6] coupled with an adaptive sampling algorithm, the LOcal Linear Approximation (LOLA)-Voronoi [10].

The MOEI criteria determines the next infill point by calculating the amount of improvement we can expect compared to the best observed objective value. In doing so, we can achieve a trade-off between exploration and exploitation of the design space. In order to maximising the model accuracy, while limiting the number of data points in an optimal manner, we employ an adaptive sampling algorithm termed the LOLA-Voronoi. This algorithm efficiently distributes new sample points in areas that highlight the most salient features of the design space. Based on the expected problem dimensionality, complexity and the form of infill strategy we wish to pursue, Kriging is a natural selection that makes the least amount of assumptions regarding the underlying landscape and provides the potential for the most accurate predication [6, 7].

This work for the first time beings together several existing techniques from different domains to provide an accessible and total approach to the design of complex metamaterial structures. This will ultimately aid in the devolvement of more complex and inhomogeneous metamaterial systems. In particular, we exploit the Kriging methodology to successfully create a Pareto-set gleamed from a 3D full-wave numerical solver suite in conjunction with a robust retrieval of effective Constitutive Parameters technique. In contrast to other optimisation strategies, we investigate the improvement in efficiency of optimisation through the use of the LOLA-Voronoi, in conjunction with Multi-Objective Constrained Expected Improvement (MOCEI). Finally, the effectiveness of the outlined algorithm will be demonstrated by a quantitative evaluation of the performance of optimised complicated magneto-electric design in the GHz regime, that current Drude-Lorentz models cannot model. The following section gives a brief overview of the components part of our optimisation scheme followed by a detailed breakdown of the multi-objective exploration of a metamaterial topology.

2. BACKGROUND

The thorough search of any highly nonlinear multi-dimensional design space inevitably requires large scale sampling. However, there are statistical approaches and adaptive sampling plans that can alleviate this impracticality. Kriging is such an approach that can build a statistical approximation of the objective landscape based on a relatively small number of observed points. Providing that the simulations are reasonably uniformly spaced, this approach will provide an accurate predication of the response of unobserved points [6, 7]. To construct a Kriging model we start with a set of n sample points, $\mathbf{X} = \left(\mathbf{x}^{(1)}, \ldots, \mathbf{x}^{(n)}\right)^T$, $\mathbf{x} \in \Re^d$. The Kriging predications $y(\mathbf{x})$ is built from a constant global model h plus a stationary Gaussian process $Z(\mathbf{x})$ representing the local deviation from the global model. The covariance matrix of $Z(\mathbf{x})$ is given by

$$\operatorname{cov}\left(Z\left(\mathbf{x}^{(i)}\right), Z\left(\mathbf{x}^{(j)}\right)\right) = \sigma^2 \Psi \tag{1}$$

where Ψ is the correlation function between any two observed points:

$$\Psi\left(\mathbf{x}^{(i)}, \mathbf{x}^{(j)}\right) = \exp\left(-\sum_{k=1}^{n} \theta_k \left\|\mathbf{x}_k^{(i)} - \mathbf{x}_k^{(j)}\right\|_k^p\right). \tag{2}$$

The hyper-parameter θ is a width parameter controlling the spatial extent of a sample points influence, and p is a parameter controlling the local smoothness[†]. A key attribute of surrogate modelling is the ability to modify the Kriging formulation such that the data can be regressed appropriately to filter out any noise. Any anomalies in the data can make optimisation difficult and might mislead an infill criteria into poor design areas. In the augmented Kriging formulation a regression constant λ is added to the leading diagonal of the correlation matrix [7]. We can now calculate the unknown hyper-parameter by maximising the ln-likelihood

$$-\frac{n}{2}\ln\left(\sigma^2\right) - \frac{1}{2}\ln\left|\det\left(\Psi + \lambda\mathbf{I}\right)\right| \tag{3}$$

where the variance and mean are given by maximum likelihood estimates (MLEs)

$$\hat{\sigma}^2 = \frac{\left(\mathbf{y} - \mathbf{1}\hat{\mu}\right)^T \left(\Psi + \lambda\mathbf{I}\right)^{-1} \Psi \left(\Psi + \lambda\mathbf{I}\right)^{-1} \left(\mathbf{y} - \mathbf{1}\hat{\mu}\right)}{n} \tag{4}$$

$$\hat{\mu} = \frac{\mathbf{1}^T \left(\Psi + \lambda\mathbf{I}\right)^{-1} \mathbf{y}}{\mathbf{1}^T \left(\Psi + \lambda\mathbf{I}\right)^{-1} \mathbf{1}}. \tag{5}$$

Equation (3) cannot be reliably solved using a local optimisation technique. As such a suitable global search routine is typically used[‡]. With the parameters estimated, the Kriging predication and corresponding estimated mean squared error (MSE) at an unknown $\mathbf{x}$ is now given by

$$\hat{y}\left(\mathbf{x}\right) = \mathbf{1}\hat{\mu} + \Psi\left(\Psi + \lambda\mathbf{I}\right)^{-1}\left(\mathbf{y} - \mathbf{1}\hat{\mu}\right) \tag{6}$$

and

$$\hat{s}^2\left(\mathbf{x}\right) = \hat{\sigma}^2\left[1 - \Psi^T\Psi^{-1}\Psi + \frac{1 - \mathbf{1}^T\Psi^{-1}\Psi}{\mathbf{1}^T\Psi^{-1}\mathbf{1}}\right]. \tag{7}$$

2.1. Infill Criteria

After building a predictive distribution model for each objective, a metric for measuring the merit of evaluating it at a new point must be decided. The success and failure of a surrogate based optimisation will rest on this choice of infill criteria that must equally balance the exploitation and exploration of a design space. By modelling the uncertainty in the predication by considering it as the realisation of a Gaussian random variable $Y\left(\mathbf{x}\right)$ with mean $\hat{y}\left(\mathbf{x}\right)$ and variance $s^2\left(\mathbf{x}\right)$, an infill criteria can be constructed which balances the values of $\hat{y}\left(\mathbf{x}\right)$ and $s^2\left(\mathbf{x}\right)$. This trade off can be successfully achieved with the Expected Improvement (EI) criteria [6, 12], which determines the next infill point by calculating the amount of improvement we can expect compared to the best observed objective value. EI is widely used in single-objective optimisation and its concept can be directly applied to multi-objective optimisation. Its equivalent, the Multi-Objective Expected Improvement (MOEI) [13], aggregates information from the independent surrogate models into a single cost function, while a max(MOEI) routine finds the new non-dominated points used to update the Pareto set. Constraints can be included in this optimisation procedure by factoring them into the calculation of the EI expectation. As with the objective function, the constrained function is modelled by a Gaussian process based on the same sampled data. Using this model to ensure that a design is feasible, we calculate the probability of the predication being greater than the constraint limit. These results are then coupled with the EI of each objective function to formulate a Multi-Objective Constrained Expected Improvement (MOCEI) by multiplying the EI by the feasibility of the constrains [7, 13]. As before the next infill point will be calculated by maximising this coupled expression to provide a new infill point.

[†] We assume that there will not be any discontinuities and use $p = 2$. Thus reducing the complexity associated with tuning the hyper-parameters.

[‡] It should be noted that for high dimensional data sets, $d > 10$, a substantial increase in computational time can occur and techniques by [11] will be required to efficiently circumvent this cost. Further reductions in time can be archived by keeping the hyper-parameter θ constant over several iterations. This has be shown to have a limited effect on the overall accuracy of the approximation.

2.2. Adaptive Sampling Plans

Employing an adaptive sampling algorithm such as the LOLA-Voronoi [10], limits the number of data points in a optimal manner while maximising model accuracy. This is achieved by balancing the trade off between exploring regions of design space not yet identified with exploitation of regions which are highly dynamic. This process starts with a initial design of experiment (DOE) sample data set, such as the Latin Hypercube (LHC) sampling technique, and uses the maximum optimality criterion of Morris and Mitchell [14] in order to achieve uniform coverage of the design space. The density of this data set is then estimated by computing an approximation of the Voronoi tessellation of the entire design space. These samples are then ranked based on the Voronoi cell size which is indicative of whether this region is under-sampled. This ensures that no region is left permanently under-sampled. An additional measure, the LOLA is now required to sample the highly dynamic regions. The LOLA component estimates the gradient at each sample location, based on a set of neighboring samples. The local nonlinearly can now be quantified from the normal of the hyperplane, which has been fitted thought the sample point based on its m neighbours in a least squared sense. Data points with a large deviation indicate a region in the design space where the data is varying more rapidly and will require a proportional increase in samples within this region. In regions where the function is almost linear, the output is easily predicted and will result in a low LOLA value. Combining the Voronoi and LOLA criteria into one metric, provides an optimal approach that can identify locations for additional points in a robust and efficient manner.

3. DISCUSSION AND RESULTS

In order to vary the effective refractive index of an artificial metallic-dielectric structure from positive to negative, careful optimisation of it constituent geometry parameters must be undertaken to ensure a specific electric and magnetic response to incident electromagnetic waves. Along with providing the required negative index values, many metamaterial-enabled devices must have minimal absorption loss. Consequently, the metallic-dielectric structures need to be optimised to give an electromagnetic response that simultaneously balances n' and n''. In order to conceptualise the complex propagation characteristics of the local field structure around metamaterial elements, one needs to average the local field charge and current distribution which yields a macroscopic interpretation of the inhomogeneous composites [15]. This homogenisation procedure relies on the applied fields having a spatial variation on a scale significantly larger than the scale of the composite particles and the period of the lattices. By replacing the inhomogeneous structure with a continuous material and restricting our analysis to that of a linear polarized incident wave, the effective permittivity ϵ and permeability μ of the inhomogeneous slab in one of its principals axis can be characterised. In this work we use a conceptually simple routine recently published [16], based on Nicolson and Ross [17] (NR) where the effective parameters are retrieved from the scattering parameters[§].

We now present our strategy to produce non-dominated Pareto sets that are well spaced on the Pareto front, which will give us a clear indication of the optimal trade-off that can be found over a range of design variables (see Table 1). While there is no hard-and-fast rule that specifies the size of the initial sampling plan (n_a^{lhc}), it is generally accepted that a minimum value of $n^{lhc_a} > 10d$, where d is the dimension of the problem, will be required to reasonably cover the d-dimensial landscape [6, 12]. The LHC sampling technique is used in conjunction with the maximum optimality criterion of Morris and Mitchell as the initial design of experiment (DOE) sample data set. The LOLA-Voronoi is next employed with a minimum value of $n_a^{lv} = n_a^{lhc}$ in order to limit the number of data points in a optimal manner while maximising model accuracy. Following this process, the location of new points of interest are iteratively found using the maximum MOCEI criteria (performed by a Hybrid Particle Swarm Optimisation algorithm (HPSO) [18]). After each iteration, the hyper-parameters are subsequently re-tuned. The tuning of the hyper-parameters is performed by a sequential GA-SQP algorithm [19] that combines the efficiency and robustness of the global search Genetic Algorithm (GA) with the fast convergence of the Sequential Quadratic Programming algorithm (SQP). After each new point is located

[§] It should be noted that in case where the dimensions of the metamaterial unit cell are approximately that of the free space wavelength, if the structure is periodic the averaging can be extended significantly beyond the usual limits of effective medium theory [15].

Table 1. Multi-objective Constrained Expected Improvement (MOCEI) algorithm, note that all design variables are normalised into the unit cube to safeguard against scaling issues.

$\mathbf{x}^r = [a^-; a^+, w^-; w^+, t_s^-; t_s^+, r^-; r^+]$
$\mathbf{x}_a = \mathbf{LatinHyperCube}\,(\mathbf{x}^r \to [0,1])$
$[\mathbf{y}_a, \mathbf{y}_b] = \mathbf{3dFEMSimulation}\,(\mathbf{x}_a \to \mathbf{x}^r)$
for $i = 1 : n_a^{lv}$
  $\mathbf{x}_a = [\mathbf{x}_a; \mathbf{LOLAVoronoi}\,(\mathbf{x}_a, \mathbf{y}_a)]$
  $[\mathbf{y}_a, \mathbf{y}_b] = [[\mathbf{y}_a, \mathbf{y}_b]; \mathbf{3dFEMSimulation}\,(\mathbf{x}_a^i \to \mathbf{x}^r)]$
endfor
$[\theta_a, \lambda_a] = \mathbf{MLE}\,(\mathbf{x}_a, \mathbf{y}_a)\,, [\theta_b, \lambda_b] = \mathbf{MLE}\,(\mathbf{x}_a, \mathbf{y}_b)$
$\widehat{R}_a = \mathbf{KrigCreate}\,(\mathbf{y}_a, \mathbf{x}_a, \theta_a, \lambda_a)\,, \widehat{R}_b = \mathbf{KrigCreate}\,(\mathbf{y}_b, \mathbf{x}_a, \theta_b, \lambda_b)$
for $j = 1 : n_a^{mocei}/4$
  for $k = 1 : 4$
    $\mathbf{x}_a = [\mathbf{x}_a; \mathbf{MOCEI}\,(\mathbf{x}_a, \mathbf{y}_a, \mathbf{y}_b)]$
    $[\mathbf{y}_a, \mathbf{y}_b] = [[\mathbf{y}_a, \mathbf{y}_b]; \mathbf{3dFEMSimulation}\,(\mathbf{x}_a^{\text{end}} \to \mathbf{x}^r)]$
  endfor
  $[\theta_a, \lambda_a] = \mathbf{MLE}\,(\mathbf{x}_a, \mathbf{y}_a)\,, [\theta_b, \lambda_b] = \mathbf{MLE}\,(\mathbf{x}_a, \mathbf{y}_b)$
  $\widehat{R}_a = \mathbf{KrigCreate}\,(\mathbf{y}_a, \mathbf{x}_a, \theta_a, \lambda_a)\,, \widehat{R}_b = \mathbf{KrigCreate}\,(\mathbf{y}_b, \mathbf{x}_a, \theta_b, \lambda_b)$
  $\mathbf{y}_{ta} = \mathbf{y}_a, \mathbf{y}_{tb} = \mathbf{y}_b, \mathbf{x}_{ta} = \mathbf{x}_a$
  for $i = 1 : \mathbf{length}(\mathbf{y}_{tb})$
    if $\mathbf{y}(i)_{tb} > \mathbf{ConstraintLimit}, \mathbf{y}(i)_{ta} = \mathbf{nan}, \mathbf{y}(i)_{tb} = \mathbf{nan}$
  endfor
  $\mathbf{x}_{ta} = \mathbf{x}_{ta}(\mathbf{find}(\sim \mathbf{isnan}(\mathbf{y}_{tb})), :), \mathbf{y}_{ta} = \mathbf{y}_{ta}(\mathbf{find}(\sim \mathbf{isnan}(\mathbf{y}_{ta})))$
  $\mathbf{y}_{tb} = \mathbf{y}_{tb}(\mathbf{find}(\sim \mathbf{isnan}(\mathbf{y}_{tb})))$
  $[\mathbf{a}, \mathbf{b}] = \mathbf{sort}(\mathbf{y}_{ta}), p = 1, \mathbf{clear\ px\ py}_a\ \mathbf{py}_b$
  $\mathbf{px}(1, 1:4) = \mathbf{x}_{ta}(\mathbf{b}(1), 1:4), \mathbf{py}_a(1) = \mathbf{y}_{ta}(\mathbf{b}(1)), \mathbf{py}_b(1) = \mathbf{y}_{tb}(\mathbf{b}(1))$
  for $i = 2 : \mathbf{length}(\mathbf{y}_{ta})$
    if $\mathbf{y}(\mathbf{b}(i))_{tb} <= \mathbf{py}(\mathbf{end})$
      $p = p + 1, \mathbf{px}(p, 1:4) = \mathbf{x}_{ta}(\mathbf{b}(i), 1:4), \mathbf{py}_a(p) = \mathbf{y}_{ta}(\mathbf{b}(i))$
      $\mathbf{py}_b(p) = \mathbf{y}_{tb}(\mathbf{b}(i))$
    endif
  endfor
  $\mathbf{plot}(\mathbf{py}_a, \mathbf{py}_b)$
endfor

and the models updated, we then sort and plot the current set of non-dominated solutions to create the Pareto front plots (see Table 1 for further details).

While the model accuracy can be assessed by using a leave-one-out cross validation procedure [7], the associated computational cost can not be warranted. Instead, the maximum MOCEI updates should proceed starting from a small initial sample size and stop when maximum MOCEI falls consecutively below a threshold over a number of iterations or when the maximum number of iterations have been met. However, in order to test the validity of the Kriging model predictions, we built a high resolution plot using 2400 (584 Latin Hypercube, 16 Corner and 1800 LOLA-Voronoi sampling plan) 3d full-wave simulations requiring a total of 112.9 hours (see Table 2). Normalised root mean squared error (RMSE) and the corresponding correlation coefficient r^2 for our Kriging predications as the number of sampling plan points is increased, expressed as a percentage of this high resolution data, are displayed in Figures 3–4. From these figure it is clear that more than 240 point are required for a reasonable global model, with RMSE $< 10\%$ and $r^2 = 0.96$. These diagrams also indicate that there is little point increasing n beyond 360 points as the surrogate model is saturated with data, and any further additions will not improve the model globally. This saturation, coupled with the relative increase in

Table 2. t_{lhlv} = total time required to simulate 240 3d full-wave simulations (54 Latin Hypercube, 16 Corner and 170 LOLA-Voronoi points), $t_{\text{in fill}}$ = total time required to MOCEI 60 infill points, t_{hy} = average time required to tune Kriging Hyper-parameters, t_t = overall time, Reference solution is composed of 2400 3d full-wave simulations (584 Latin Hypercube, 16 Corner and 1800 LOLA-Voronoi points).

Symbol	2d Pareto front solution	Reference solution
a (mm)	$4.5 \rightarrow 5.0$	-
w (mm)	$1.5 \rightarrow 2.0$	-
r (mm)	$1.75 \rightarrow 2.25$	-
t_s (mm)	$0.7 \rightarrow 1.2$	-
t_m (mm)	0.01335	-
t_{lhlv} (sec)	45356	-
$t_{\text{in fill}}$ (sec)	31316	-
t_{hy} (sec)	341	-
t_t (sec)	76672 (21.3 hrs)	406475 (112.9 hrs)

computational expense, as illustrated in Figure 5, sets a natural limit on the size of the model n.

3.1. Isotropic Fishnet Metamaterial Design

In this study, we consider the application of the proposed topology optimisation strategy to examine the range of optimal negative refractive indices that can be achieved using the fishnet metamaterial structure, as shown in Figures 1, 2 and experimentally demonstrated in [20]. The objective of this optimisation will be to produce a set of non-dominated Pareto sets that are well spaced on the Pareto front which will give us a clear indication of the optimal trade-off between n' and n'' at 40 GHz, that can be found over a range of design variables. In particular, the structure is parameterised by $d = 4$ design variable whose ranges $\mathbf{x}^r$ are given in Table 2. The structures substrate is Duroid 5880 ($\epsilon = 2.2$,

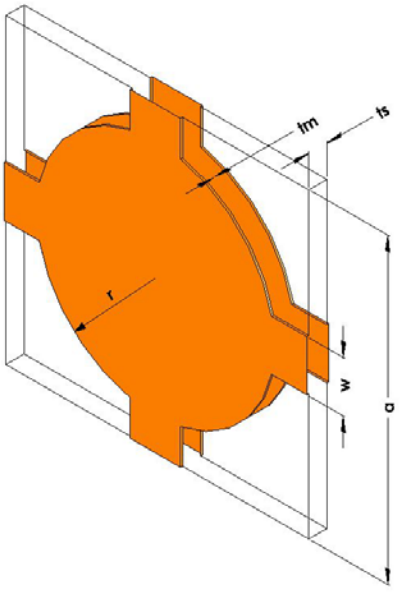

Figure 1. Schematic representation of the 2D isotropic fishnet metamaterial design.

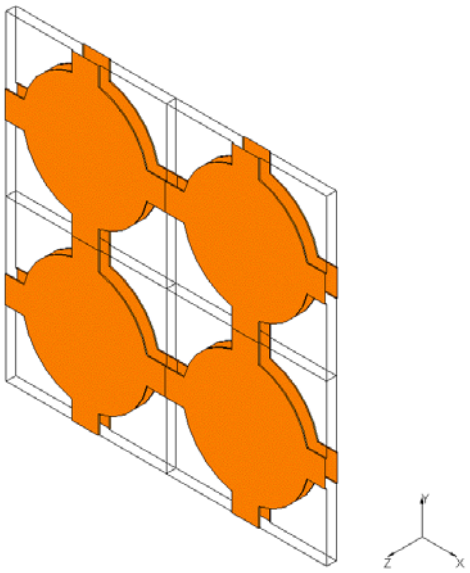

Figure 2. Isometric view of a layer of the metamaterial consisting of a fishnet layer separated by a thin dielectric substrate.

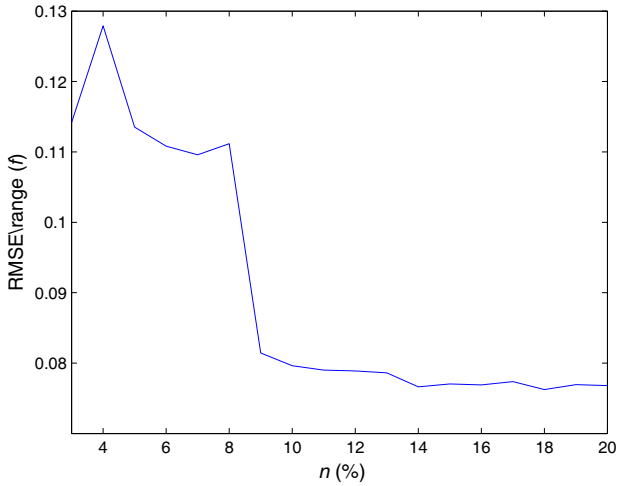

Figure 3. Normalised RMSE for a Kriging predication as the number of sampling plan points is increased (expressed as a percentage of the simulated test data).

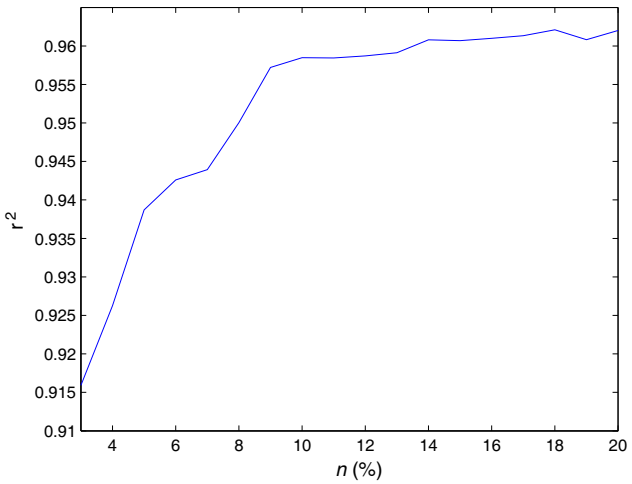

Figure 4. The correlation coefficient r^2 for a Kriging predication as the number of sampling plan points is increased.

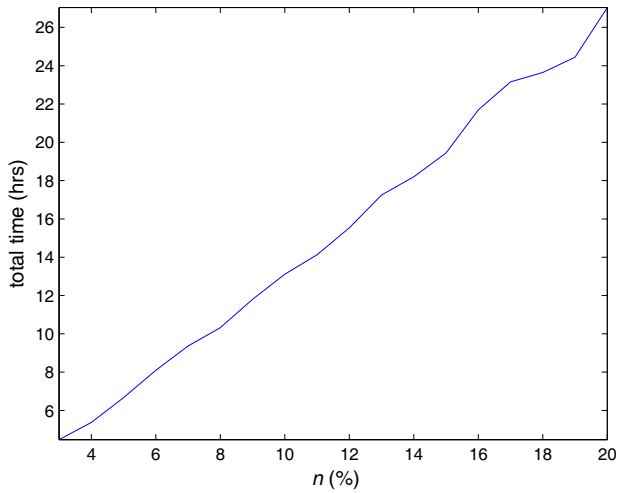

Figure 5. Total time required to simulate and create a Kriging meta-model as the number of sampling plan points is increased.

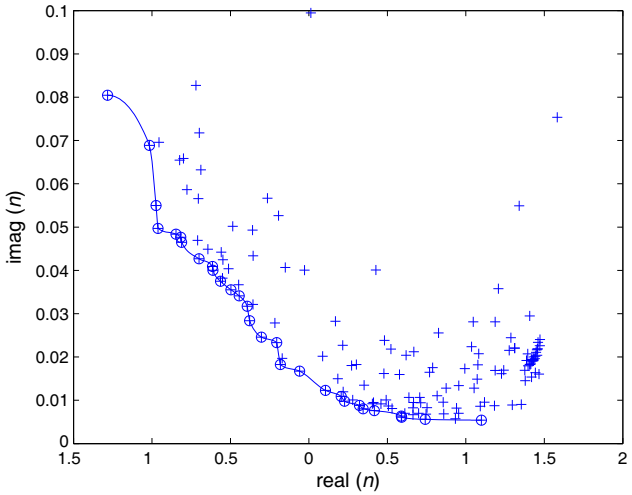

Figure 6. 2d Pareto front generated composed of a total of 29 non-dominated designs.

loss tangent $\delta = 0.0009$ at 40 GHz) separating two copper layers of thickness t_m. Periodic magnetic and electric boundary conditions are placed in the x and y planes respectively, and a 1 mm thick air layer is placed on either side of the structure in the z plane which constitutes the effective boundaries between the metamaterial slab and air. The data is simulated in CST Microwave Studio subject to a $1e^{-5}$ Tetrahedral mesh accuracy employing a 3rd order solver, which resulted in an average simulation time of 215 seconds. In addition to reduced undesired absorption, we restricted the refractive indices with imaginary parts to be smaller than 0.1 incorporating this constraint into our optimisation scheme is achieved by using the MOCEI as detailed earlier. To produce the non-dominated designs, we used a 54-point Latin Hypercube and 16-point corner sampling plan, augmented with 170-point derived from the LOLA-Voronoi process. A further 60 points were then sampled using the maximum MOCEI criteria.

Figure 6 shows the 29 non-dominated solutions and associated Pareto front found using this infill strategy. It is clear that relative uniform spread of optimal trade-off designs have been found over

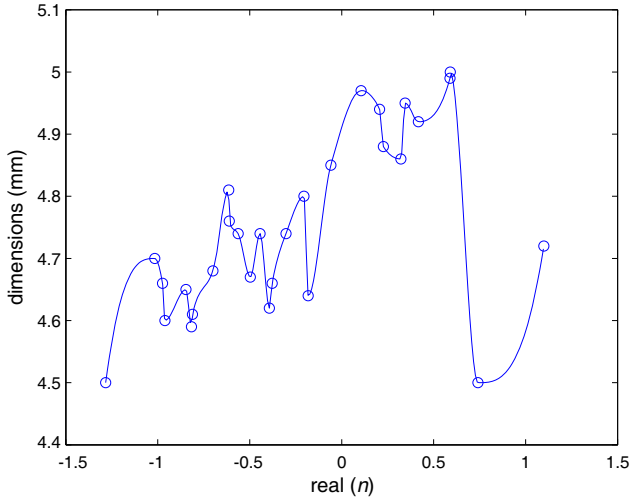

Figure 7. Corresponding design variable a dimensions for 2d Pareto front.

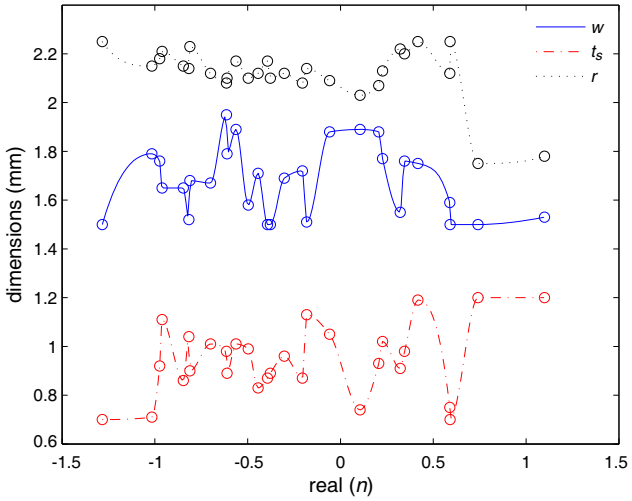

Figure 8. Corresponding design variables w, t_s, r dimensions for 2d Pareto front.

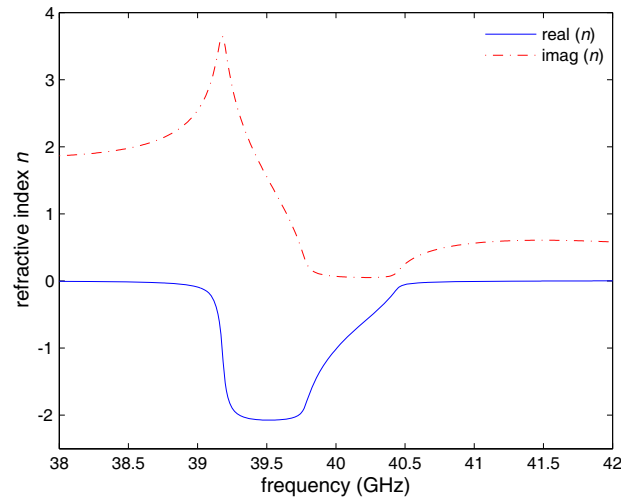

Figure 9. Refractive index simulation of optimum Pareto front design $\mathbf{x}^* = [4.7, 1.79, 0.71, 2.15]$, $n = -1.016 + 0.068i$ at 40 GHz.

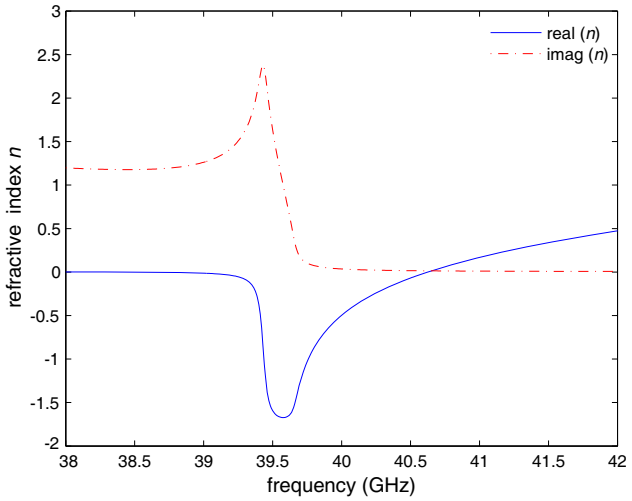

Figure 10. Refractive index simulation of optimum Pareto front design $\mathbf{x}^* = [4.67, 1.58, 0.99, 2.1]$, $n = -0.497 + 0.035i$ at 40 GHz.

the entire n' range $[-1 \ +1]$ indicating that the MOCEI has successfully balanced the exploration and exploitation of the Pareto front. Included in this figure are the full range of solution that fulfilled the constraint criteria but didn't form the final Pareto front. In addition, the corresponding design variable dimensions for the Pareto front are displayed in Figures 7 and 8, which provide a designer invaluable insight into the complicated interactions of these magneto-electric designs. The resulting retrieved effective medium properties from two of these Pareto sets, determined by our optimisation strategy, can be examined in Figures 9 and 10.

The advantage of the LOLA-Voronoi is demonstrated in not just avoiding sampling sub-optimal regions, but one which can produce a significant reduction in computational time as a consequence of requiring less maximum CEI global searches in determining the new sample points. Compared with directly searching the objective and constraint functions using a multi-objective search algorithm, the possible benefits are clearly evident. Our strategy requiring just 360 simulations, as apposed to typically thousands of calls required with traditional approaches (see Table 2).

4. CONCLUSIONS

In this work, we proposed an efficient and automated optimisation approach, which exploits the Kriging methodology in conjunction with the LOLA-Voronoi and MOCEI to design and optimise complex and inhomogeneous metamaterial structures. This approach overcomes the limitations of conventional approaches which directly search the objective and constraint functions using a multi objective search algorithm, resulting in drastically reduced simulation times that might otherwise be impractical. By coupling this optimisation approach with a 3D full-wave numerical solver suite and a robust retrieval of effective constitutive parameter technique, we have shown how one can simultaneously optimise the real and imaginary component of the refractive index in an optimal sense to create a set on non-dominating Pareto solutions. Finally, the effectiveness of the outlined algorithm was demonstrated by a quantitative evaluation of the performance of optimised planar 2D negative refractive index structures in the GHz regime.

REFERENCES

1. Cui, T. J., D. Smith, and R. Liu, *Metamaterials: Theory, Design, and Applications*, 1st Edition, Springer Publishing Company, Incorporated, 2009.
2. Fang, F., Y. Cheng, and H. Liao, "Numerical study on a three-dimensional broadband isotropic left-handed metamaterial based on closed rings," *Physica Scripta*, Vol. 89, No. 2, 025501, 2014.
3. Bradley, P. J., "A multi-fidelity based adaptive sampling optimisation approach for the rapid design of double-negative metamaterials," *Progress In Electromagnetics Research B*, Vol. 55, 87–114, 2013.
4. Wagner, T., M. Emmerich, A. Deutz, and W. Ponweiser, "On expected-improvement criteria for model-based multi-objective optimization," *Parallel Problem Solving from Nature*, Vol. 6238, 718–727, Springer, Berlin, Heidelberg, 2010.
5. Wilson, B., D. Cappelleri, T. W. Simpson, and M. Frecker, "Efficient pareto frontier exploration using surrogate approximations," *Optimization and Engineering*, Vol. 2, No. 1, 31–50, 2001.
6. Jones, D. R., "A taxonomy of global optimization methods based on response surfaces," *Journal of Global Optimization*, Vol. 21, No. 4, 345–383, 2001.
7. Forrester, A., A. Sobester, and A. Keane, *Engineering Design via Surrogate Modelling: A Practical Guide*, Wiley, 2008.
8. Mohan, M., K. Deb, and S. Mishra, "Evaluating the Edomination based multi-objective evolutionary algorithm for a quick computation of Pareto-optimal solutions," *Evolutionary Computation*, Vol. 13, No. 4, 501–525, 2005.
9. Martinez-Iranzo, M., J. M. Herrero, J. Sanchis, X. Blasco, and S. Garcia-Nieto, "Applied Pareto multi-objective optimization by stochastic solvers," *Engineering Applications of Artificial Intelligence*, Vol. 22, No. 3, 455–465, 2009.
10. Deschrijver, D., K. Crombecq, H. M. Nguyen, and T. Dhaene, "Adaptive sampling algorithm for macromodeling of parameterized S-parameter responses," *IEEE Transactions on Microwave Theory and Techniques*, Vol. 59, No. 1, 39–45, Jan. 2011.
11. Toal, D. J. J., A. I. J. Forrester, N. W. Bressloff, A. J. Keane, and C. Holden, "An adjoint for likelihood maximization," *Proceedings of the R*, Vol. 465, No. 2111, 3267–3287, Nov. 2009.
12. Jones, D. R., M. Schonlau, and W. J. Welch, "Efficient global optimization of expensive black-box functions," *Journal of Global Optimization*, Vol. 13, No. 4, 455–492, Dec. 1998.
13. Keane, A., "Statistical improvement criteria for use in multiobjective design optimization," *AIAA Journal*, Vol. 44, No. 4, 879–891, 2006.
14. Morris, M. D. and T. J. Mitchell, "Exploratory designs for computational experiments," *Journal of Statistical Planning and Inference*, Vol. 43, No. 3, 381–402, 1995.
15. Smith, D. R., D. C. Vier, Th. Koschny, and C. M. Soukoulis, "Electromagnetic parameter retrieval from inhomogeneous metamaterials," *Phys. Rev. E*, Vol. 71, 036617, Mar. 2005.

16. Barroso, J. J. and U. C. Hasar, "Constitutive parameters of a metamaterial slab retrieved by the phase unwrapping method," *Journal of Infrared, Millimeter, and Terahertz Waves*, Vol. 33, No. 2, 237–244, 2012.
17. Nicolson, A. M. and G. F. Ross, "Measurement of the intrinsic properties of materials by time-domain techniques," *IEEE Transactions on Instrumentation and Measurement*, Vol. 19, No. 4, 377–382, 1970.
18. Yu, S., Z. Wu, H. Wang, and Z. Chen, "A hybrid particle swarm optimization algorithm based on space transformation search and a modified velocity model," *High Performance Computing and Applications*, Vol. 5938, 522–527, 2010.
19. Mansoornejad, B., N. Mostoufi, and F. Jalali-Farahani, "A hybrid GA-SQP optimization technique for determination of kinetic parameters of hydrogenation reactions," *Computers & Chemical Engineering*, Vol. 32, No. 7, 1447–1455, 2008.
20. Zaoui, W. S., K. Chen, W. Vogel, and M. Berroth, "Low loss broadband polarization independent fishnet negative index metamaterial at 40 GHz," *Photonics and Nanostructures — Fundamentals and Applications*, Vol. 10, No. 3, 245–250, 2012.